

# Reversible Restricted Diffusion in the Corpus Callosum in Various Pediatric Diseases<sup>1</sup>

소아 질환에서 나타나는 뇌량의 가역적 확산강조영상 소견<sup>1</sup>

Won Kyung Kim, MD<sup>1</sup>, Hyun Sook Hong, MD<sup>1</sup>, A Leum Lee, MD<sup>1</sup>, Jang Gyu Cha, MD<sup>1</sup>, Hae Kyung Lee, MD<sup>1</sup>, Won Kyung Bae, MD<sup>2</sup>

<sup>1</sup>Department of Radiology, Soonchunhyang University Bucheon Hospital, Soonchunhyang University College of Medicine, Bucheon, Korea

<sup>2</sup>Department of Radiology, Soonchunhyang University Cheonan Hospital, Soonchunhyang University College of Medicine, Cheonan, Korea

**Purpose:** To evaluate the reversible restricted diffusion in the corpus callosum in pediatric patients with clinical findings, and to discuss the possible pathogenesis of these lesions.

**Materials and Methods:** Between 2007 and 2011, seven children with reversible signal abnormalities in the corpus callosum were identified and retrospectively reviewed.

**Results:** Diseases and conditions associated with lesions included: trauma ( $n = 3$ ), neonatal seizure ( $n = 1$ ), clinically suspected mild encephalopathy ( $n = 1$ ), multiple sclerosis ( $n = 1$ ), and seizure with subdural hygroma ( $n = 1$ ). The callosal lesions were located in the splenium and the genu ( $n = 2$ ), the splenium and the body ( $n = 1$ ), and the splenium only ( $n = 4$ ). The shape of the lesions was round-to-ovoid ( $n = 4$ ) or linear ( $n = 3$ ). Follow-up MRI scans showed completely resolved ( $n = 6$ ) or persistent ( $n = 1$ ) signal abnormalities on diffusion-weighted imaging as well as apparent diffusion coefficient mapping. Clinical outcomes were good in six of the patents but poor in the seventh.

**Conclusion:** Reversible restricted diffusion in the corpus callosum can develop in various diseases. Knowledge of the MRI findings and associated diseases might be helpful in predicting patients' conditions and clinical outcomes.

## Index terms

Corpus Callosum

Splenium

Diffusion-Weighted Imaging

Magnetic Resonance Imaging

Diffuse Axonal Injury

Cytotoxic Edema

**Received** December 23, 2011;

**Accepted** February 6, 2012

**Corresponding author:** Hyun Sook Hong, MD  
Department of Radiology, Soonchunhyang University  
Bucheon Hospital, Soonchunhyang University College of  
Medicine, 170 Jomaru-ro, Wonmi-gu, Bucheon 420-  
767, Korea.

Tel. 82-32-621-5851 Fax. 82-32-621-5874

E-mail: hshong@schmc.ac.kr

Copyrights © 2012 The Korean Society of Radiology

## INTRODUCTION

The corpus callosum (CC), the main tract connecting the two cerebral hemispheres, forms the largest commissural white matter bundle in the brain, with some 200 million axons (1). The structural role of the CC is the interhemispheric transfer of auditory, visual, sensory, and motor information relevant to multiple cognitive processes (1).

Reversible restricted diffusion in the corpus callosum has been found to be associated with the administration or rapid withdrawal of antiepileptic drugs in patients with seizure, infectious encephalopathy such as influenza, rotavirus, or O-157 *Escherichia coli*, neonatal hypoglycemia, multiple sclerosis (MS), trauma, and drug toxicity (1-10). According to a previ-

ous report, complete clinical regression of the underlying diseases or conditions leads to the disappearance of these lesions (11).

The purpose of this study is to evaluate the reversible restricted diffusion in the corpus callosum in pediatric patients with clinical findings and to discuss the possible pathogenesis of these lesions.

## MATERIALS AND METHODS

### Patients

Between January 2007 and November 2011, 9933 pediatric patients underwent brain MRI in two tertiary university hospitals in Korea. We recruited 27 patients who revealed restricted

diffusion in the CC. Among them, 7 who underwent follow-up MRI were enrolled in the study. The MRI results of 7 of the cases (five boys and two girls; age range, 0-19 years; mean age, 8.6 years) were retrospectively reviewed with patients' symptoms, clinical histories, medications, laboratory findings, clinical diagnoses, and prognoses.

### MR Imaging and Image Analysis

All scanning was performed using a 1.5 T or 3.0 T MRI scanner (Signa HDxt; GE Healthcare, Milwaukee, WI, USA) in one hospital and a 1.5 T MRI scanner (Gyrosan Intera; Philips Healthcare, Las Vegas, NV, USA) or 3.0 T MRI scanner (Achieva; Philips Healthcare) in the other. Sedating agents were used when necessary. The MRI protocol included T1-weighted (T1-W) spin-echo with or without contrast agents, T2-weighted (T2-W) fast spin-echo, fluid-attenuated inversion-recovery (FLAIR), diffusion-weighted imaging (DWI), and apparent diffusion coefficient (ADC) mapping. Diffusion-weighted images were acquired at a b value of 1000 s/mm<sup>2</sup>.

Magnetic resonance (MR) images of all these children were assessed by two experienced board-certified pediatric neuroradiologists and one resident. All images were reviewed individually. We defined reversible restricted diffusion in the CC as high signal intensity (SI) lesions on DWI and low SI lesions on an ADC map in the CC, with or without corresponding signal changes on T1-W, T2-W, or FLAIR images, which had disappeared on all sequences during the follow-up study. Upon follow-up MRI, we analyzed MRI findings, such as location and shape of the CC lesions, signal abnormalities on DWI, and an ADC map with signal changes. Conventional T1- and T2-W images were reviewed to assess pre- and coexisting parenchy-

mal lesions or other brain diseases. Additionally, clinical diagnoses and outcomes were reviewed and compared to the MRI findings for the seven patients.

## RESULTS

### Clinical Outcome of Patients

Table 1 lists the details of the clinical data for the seven patients. Clinical data were analyzed retrospectively, with particular attention to identifying the etiology of the lesions. The children's symptoms, which prompted MRI, included: drowsy to stuporous mentality in three of the patients (cases 1-3), seizures in two (cases 4, 7), headache with fever in one (case 5), and nausea with vomiting in another (case 6). Diseases and conditions associated with the lesions included trauma in three patients (cases 1-3), neonatal seizure (case 4), clinically suspected mild encephalopathy (case 5), MS (case 6), and seizure with subdural hygroma (case 7). Clinical outcomes were good in six patients (cases 1-6), but poor in one (case 7).

### MRI Findings

Table 2 lists the details of MRI findings for the seven patients.

### Location and Shape

The callosal lesions were located in both the splenium and the genu in two patients (cases 1, 2) (Fig. 1), the splenium and the body in one patient (case 3) (Fig. 2), and the splenium only in four patients (cases 4-7) (Figs. 3-6). All of the cases involved the splenium. The shape of the lesion was round-to-ovoid in four patients (cases 1, 3, 5, 6) (Figs. 1, 2, 4, 5) and linear in three patients (cases 2, 4, 7) (Figs. 3, 6).

**Table 1. Summary of Clinical Data for Patients with Corpus Callosum Lesions**

Patient No.	Age/Gender	Initial Symptom	Diseases and Conditions	Treatment	Clinical Outcome
1	4 yr/M	Drowsy mentality	Trauma by TA	Conservative	Good
2	9 yr/M	Drowsy mentality	Trauma by TA	Conservative	Good
3	14 yr/F	Stuporous mentality	Trauma by TA	Conservative	Good
4	3 d/M	Seizure	Neonatal seizure	Phenobarbital	Good
5	14 yr/M	Headache, fever	Clinically mild encephalopathy	Vancomycin	Good
6	19 yr/M	Nausea, vomiting	Multiple sclerosis	Steroid pulse therapy with interferon	Relapsing and remitting
7	3 mo/F	Repeated seizures	Seizure with subdural hygroma	Phenobarbital and phenytoin	Burr-hole drainage due to aggravated subdural hygroma

Note.—d = day, F = female, M = male, mo = months, No = number, TA = traffic accident, yr = years

**Table 2. MRI Findings for Patients with Corpus Callosum Lesions**

Patient No.	Initial MRI	Location	Shape	DWI	ADC	T2-WI or FLAIR	T1-WI	Other Lesions	Follow-Up MRI; Interval between Initial MRI
1	7 d	Splenium and genu	Tiny ovoid	H	L	H	L	Subdural hygroma and hemorrhagic foci	6 mo
2	10 d	Splenium and genu	Linear	H	L	H	L	Hemorrhagic foci in both frontal lobes	2 mo
3	9 d	Splenium and body	Round	H	L	H	L	Hemorrhagic contusion in left frontal lobe	17 mo
4	2 d	Splenium	Linear	H	L	I	I	Microhemorrhage in both parietal lobes	17 d
5	2 d	Splenium	Round	H	I	H	L	(-)	1 mo
6	1 d	Splenium	Round	H	L	H	L	Multiple sclerosis involving BG, PVWM of left parietal lobe	17 mo
7	6 d	Splenium	Linear	H	L	H	L	Subdural hygroma	1 mo

Note.—ADC = apparent diffusion coefficient, BG = basal ganglia, d = days, DWI = diffusion-weighted imaging, FLAIR = fluid-attenuated inversion-recovery, H = high signal, I = iso-signal, L = low signal, mo = months, No = number, PVWM = periventricular white matter, W = weighted image, - = negative finding

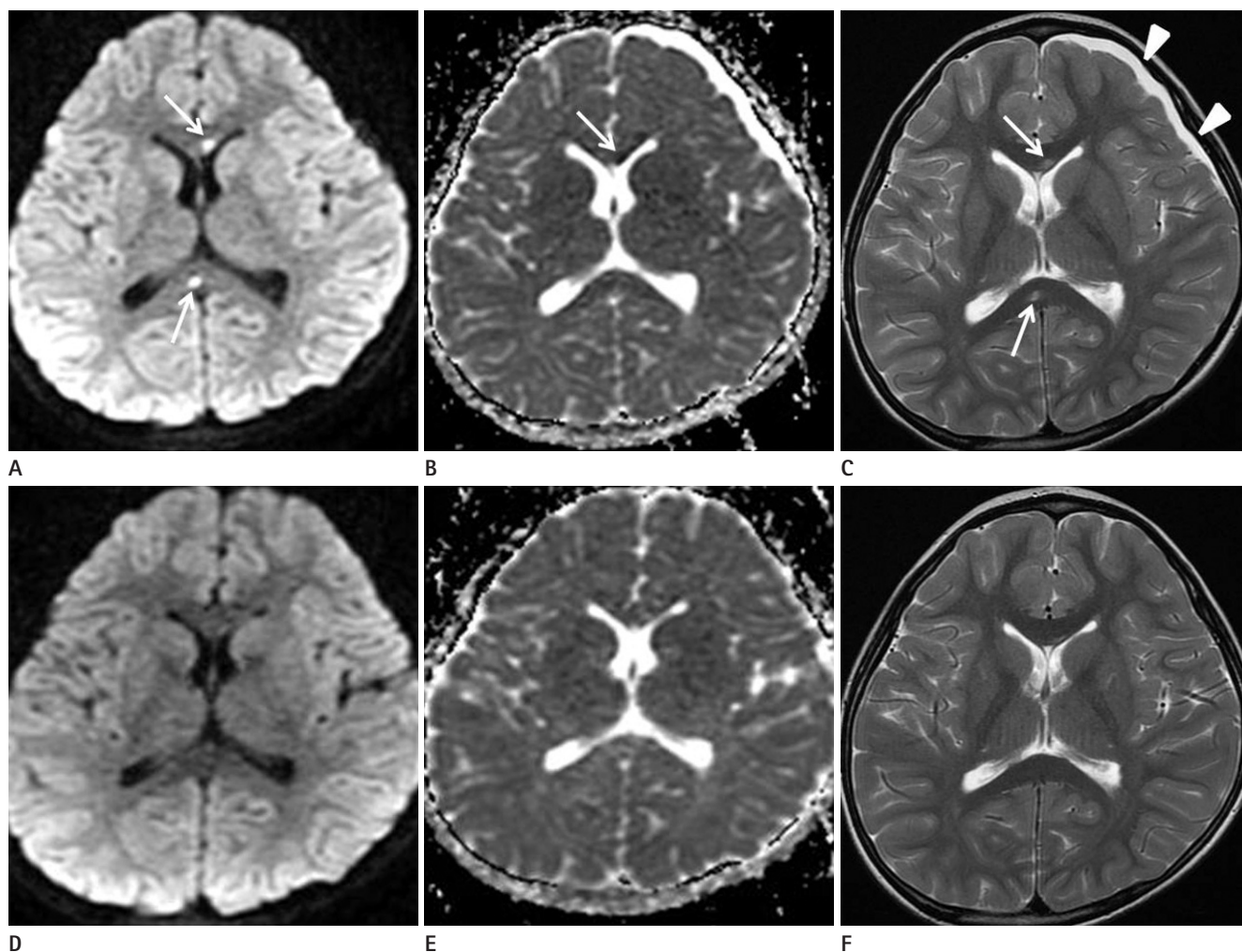


**Fig. 1.** A 4-year-old boy with drowsy mentality caused by motorcar accident (case 1). Initial MRI (A–C) shows well-defined, tiny, ovoid-shaped bright SI lesions (arrows) on DWI (A) in the genu and the splenium, dark SI (arrow) on an ADC map (B) in the genu of the corpus callosum. T2-WI (C) shows high SI lesions in the genu and the splenium (arrows) and crescentic subdural hygroma in the left frontal region (arrowhead). Multiple hemorrhagic foci were observed in the left cerebellum and pons, on gradient echo imaging, and cerebral contusions were observed in the right frontal and left parietal lobes (not shown). Follow-up MRI (D–F) after 6 months shows complete resolution of signal abnormalities on all sequences.

Note.—ADC = apparent diffusion coefficient, DWI = diffusion-weighted imaging, SI = signal intensity, T2-WI = T2-weighted image

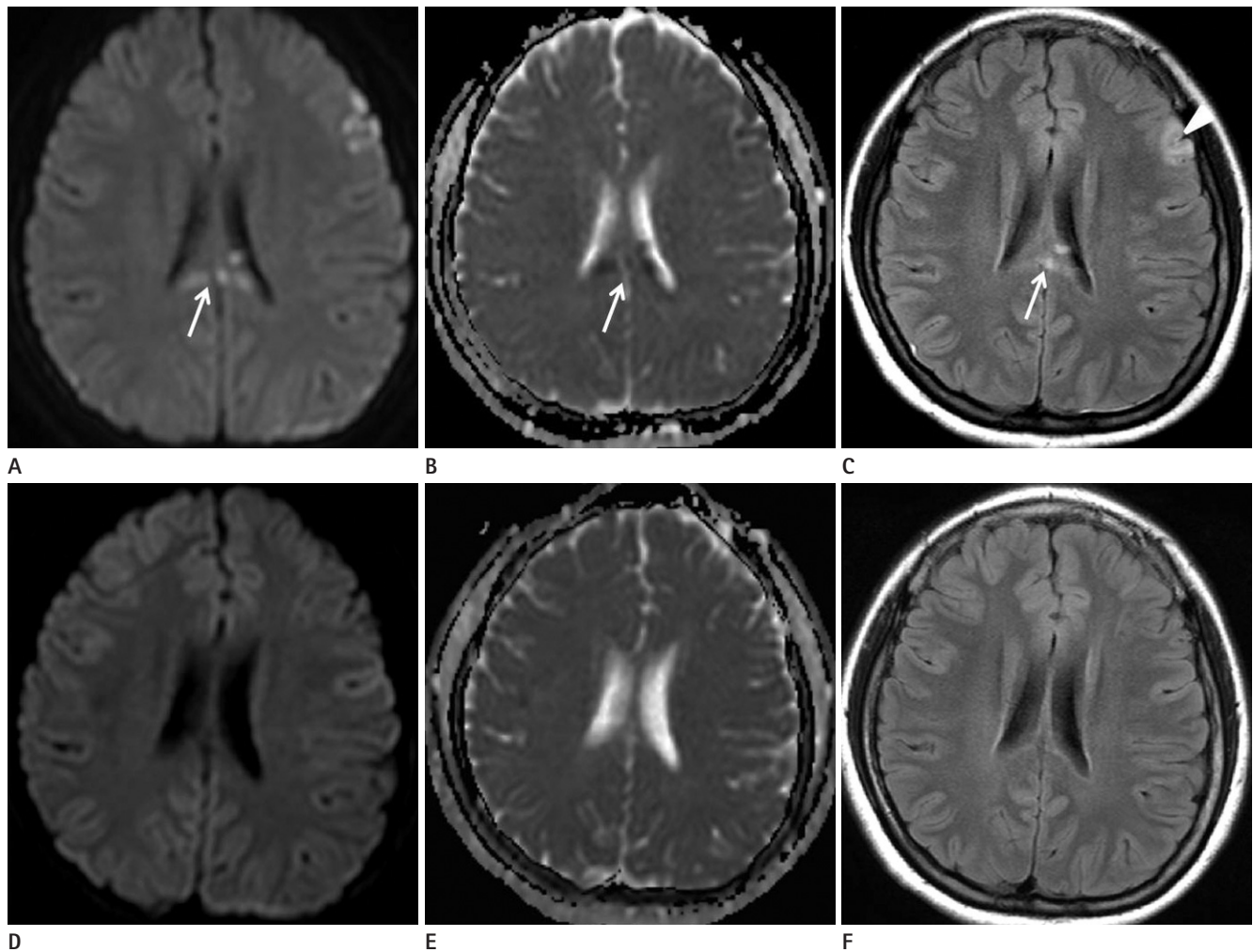


**Fig. 2.** A 14-year-old girl with stuporous mentality following a motorcycle traffic accident (case 3). Initial MRI (**A–C**) shows multifocal nodular high SI lesions (arrow) on DWI (**A**) and low SI (arrow) on an ADC map (**B**) in the splenium and the body of the corpus callosum. FLAIR imaging (**C**) shows high SI lesions in the splenium and the body (arrow), with hemorrhagic contusion in the left frontotemporal cortex (arrowhead). Follow-up MRI (**D–F**) after 17 months shows complete resolution of signal abnormalities on all sequences. Note.—ADC = apparent diffusion coefficient, DWI = diffusion-weighted imaging, FLAIR = fluid-attenuated inversion-recovery, SI = signal intensity

### Signal Abnormalities

All patients exhibited a high SI on DWI, while six of the seven showed a low SI on the ADC map in the CC (Figs. 1-6). Only one patient (case 5) showed an iso-SI on an ADC map (Fig. 4B). The ADC value was not evaluated because all cases were evaluated retrospectively. On axial T1- or T2-W and FLAIR images, six of the seven patients showed a high SI on T2-WI or FLAIR image and a low SI on T1-WI, except for one patient (case 4), who showed no obvious signal abnormality on T2-WI (Fig. 3C).

### Other Parenchymal Lesions

Regarding these case series, an isolated corpus callosum lesion was apparent in only one case of clinically suspected mild

encephalopathy (case 5) (Fig. 4). Other parenchymal lesions were found in six cases. In the trauma cases (cases 1-3), crescentic subdural hygroma (Fig. 1C), multiple hemorrhagic foci, and contusions were observed in brain parenchyma (Fig. 2C). In the patient with neonatal seizure (case 4), crescentic subdural hemorrhage was observed along the tentorium and interhemispheric fissure (not shown). In the patient with MS (case 6), multifocal nodular high SI lesions were observed in both thalami, the right caudate nucleus, and the periventricular white matter of the left parietal lobe (Fig. 5C). In case 7, crescentic subdural hygroma was observed in both frontotemporoparietal regions (Fig. 6C). Additionally, ill-defined high SI lesions on DWI, with subtle cortical sulcal effacement, were present in

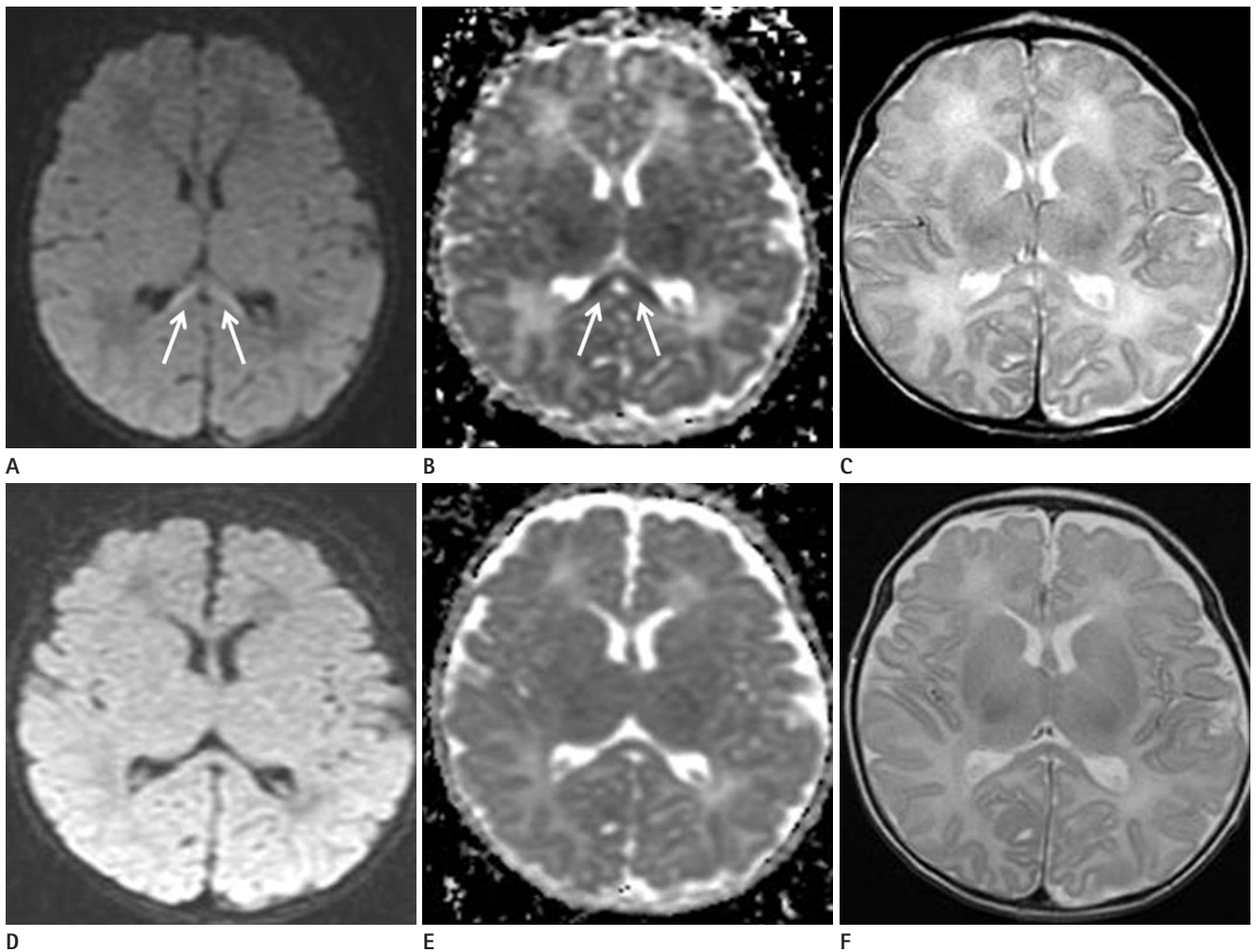


**Fig. 3.** A male infant with clonic seizures (case 4). Initial MRI (**A–C**) shows bilateral linear high SI lesions (arrows) on DWI (**A**) and low SI (arrows) on an ADC map (**B**) in the splenium of the corpus callosum. On T2-WI (**C**), the signal abnormality is not obvious. Additionally, crescentic subdural hemorrhage was observed along the tentorium and interhemispheric fissure (not shown). Follow-up MRI (**D–F**) after 17 days (20 days of age), shows resolution of signal abnormalities on DWI (**D**) and an ADC map (**E**). Follow-up T2-WI (**F**) also shows no signal abnormality. Note.—ADC = apparent diffusion coefficient, DWI = diffusion-weighted imaging, SI = signal intensity, T2-WI = T2-weighted image

both occipital lobes (Fig. 6A), without low SI on ADC map, suggesting vasogenic edema.

#### Follow-Up MRI

The interval between the initial and follow-up MRI scans ranged from 17 days to 17 months. Upon follow-up MRI, six patients showed complete resolution of signal abnormalities in the corpus callosum (cases 1-6), whereas, in one patient, the restricted diffusion in the corpus callosum was persistent (case 7) (Fig. 6D, E).

## DISCUSSION

The CC is the second most common area involved in diffuse

axonal injury (21-47%). The CC is considered particularly vulnerable to trauma because of its unique location and composition (1). The CC comprises dense myelinated fibers relative to the adjacent hemispheric white matter. This densely compacted nature of the white matter tracts renders it susceptible to shear injury in the event of trauma. The callosal lesions most commonly involve the splenium; they are typically eccentric in location and can involve a focal part or the full thickness of the CC (9). This is thought to be a diffuse axonal injury due to axonal stretching by forces of inertia.

Seizures induce cellular swelling and fluctuations in extracellular water (12). Several studies have reported possible etiologic explanations for restricted diffusion in the CC, such as cytotoxic

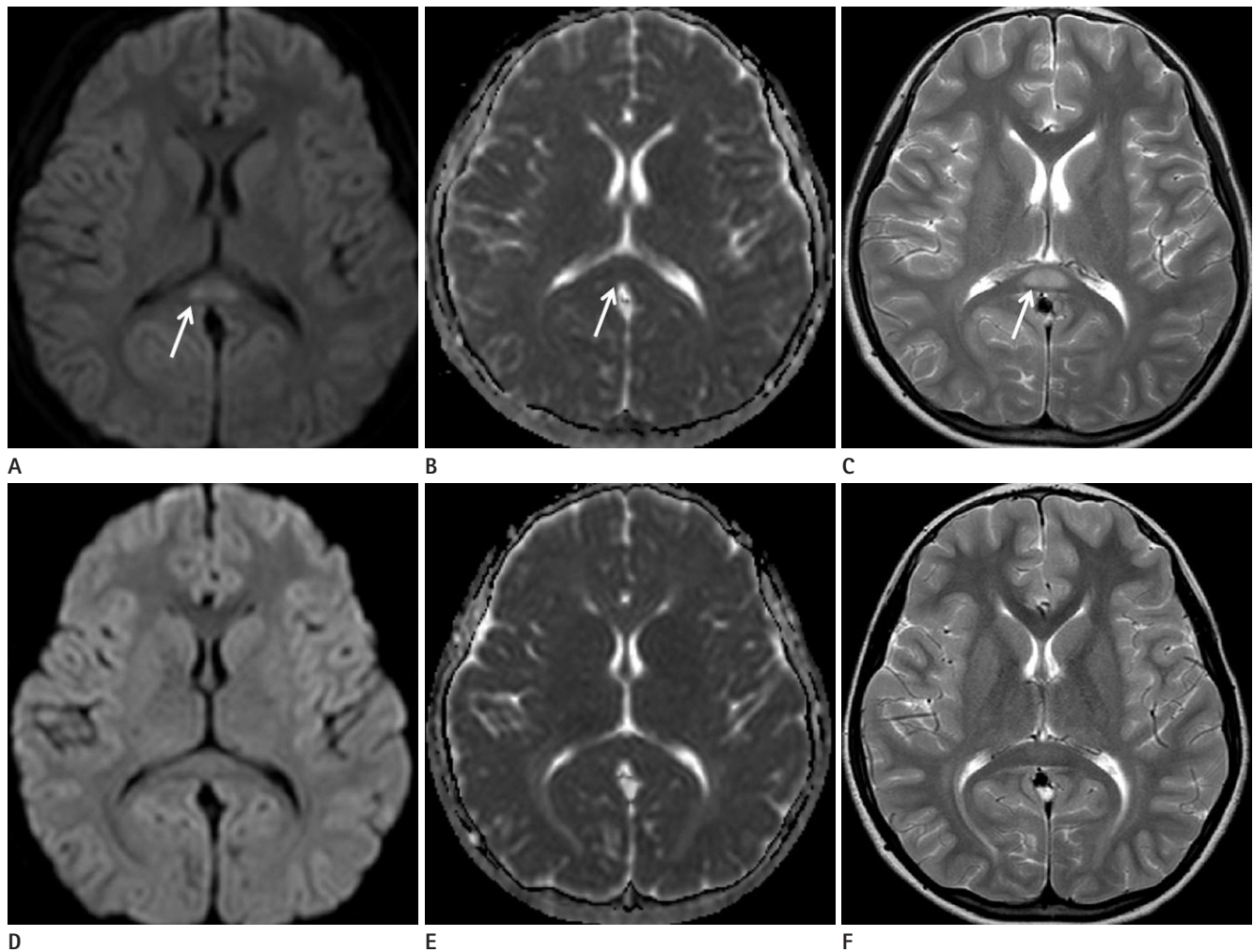


**Fig. 4.** A 14-year-old boy with headache and fever (case 5). Initial MRI (**A-C**) shows ovoid high SI lesion (arrow) on DWI (**A**) and iso-SI (arrow) on an ADC map (**B**) in the central portion of the splenium. T2-WI (**C**) shows well-defined, ovoid, high SI (arrow) in the splenium of the corpus callosum. Follow-up MRI (**D-F**), after 1 month, shows resolution of signal abnormalities on all sequences.  
 Note. —ADC = apparent diffusion coefficient, DWI = diffusion-weighted imaging, SI = signal intensity, T2-WI = T2-weighted image

ic edema secondary to seizure spread (3), reversible demyelination related to the toxicity of antiepileptic drugs (2), or secondary to arginine vasopressin imbalance induced by rapid antiepileptic drug change (2, 4). In our neonatal patient (case 4), MRI was performed on the second day, immediately after administration of phenobarbital. Thus, her seizure was most likely a factor contributing to the DWI signal change, although the antiepileptic drug might have also caused the signal abnormalities. However, several reports exist regarding seizure with antiepileptic treatment in adult patients, but only a few reports can be found which concern seizure in neonate patients (13, 14). Our patient, 2 days old, (case 4) was also a neonate. The mechanism of the abnormal DWI findings in the neonate is unknown. The reduced ADC suggests cytotoxic edema, but

our case did not suggest neonatal hypoxic-ischemic injury because basal ganglia and thalami were spared, and his prognosis was excellent after conservative treatment. Pathologically, myelination of the splenium does not occur before 2 months of age. Thus, intramyelinic edema is not responsible for these reversible callosal lesions (13). Another theory is interstitial edema. Because axons in the CC are the most tightly packed axons in the brain, interstitial edema in the extracellular space between the unmyelinated axons might cause restricted diffusion (15). Thus, in patients with general seizure, cytotoxic edema due to seizure or reversible demyelination related to the toxicity of antiepileptic drugs might be the most probable mechanism, whereas interstitial edema might be considered in neonates.

Certain drugs and viral infections are suspected to cause cy-

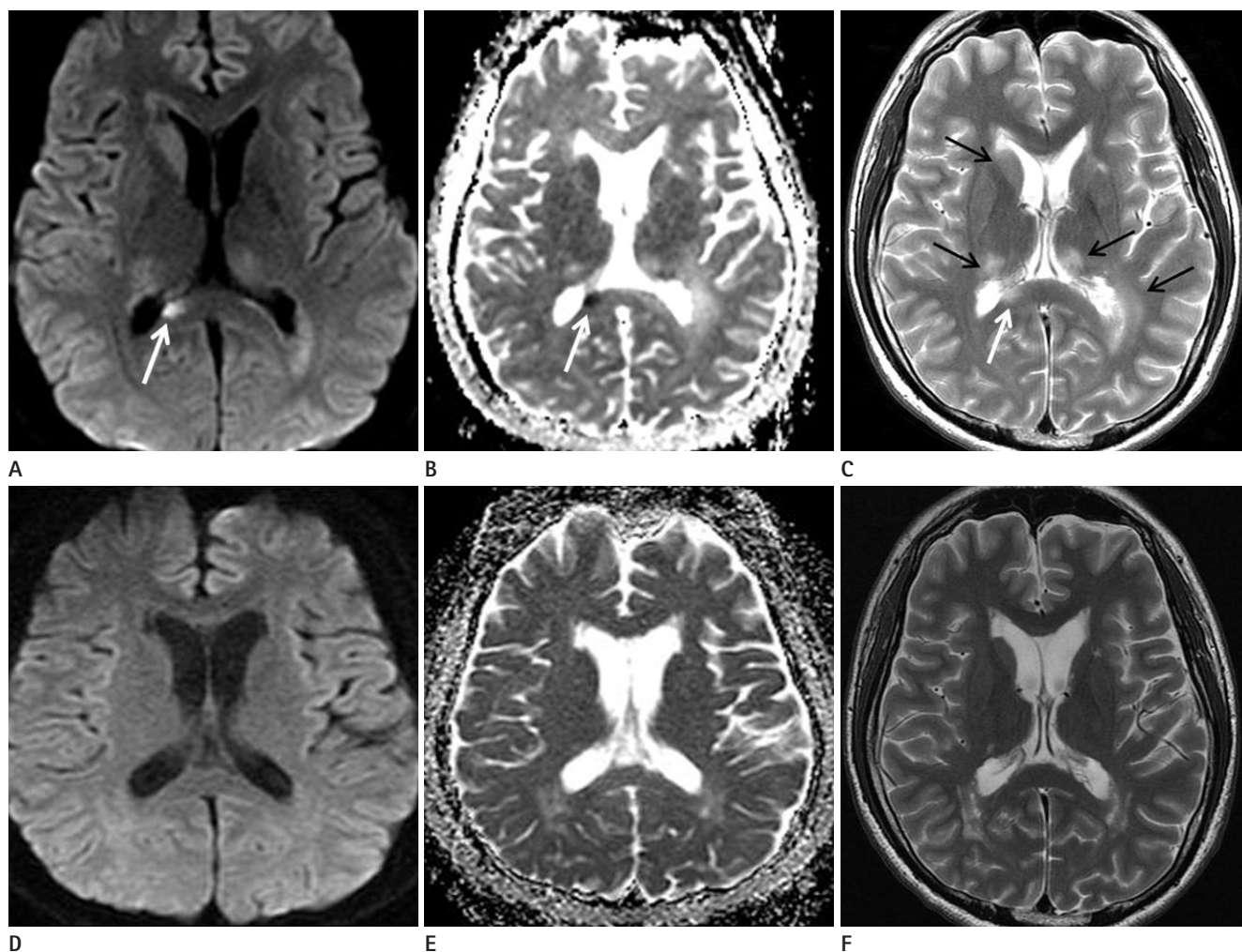


**Fig. 5.** A 19-year-old man with a history of multiple sclerosis (case 6) experienced nausea and vomiting. Initial MRI (**A–C**) shows focal, nodular, bright SI lesion (arrow) on DWI (**A**) and dark SI (arrow) on an ADC map (**B**) in the right lateral aspect of the splenium. T2-WI (**C**) shows high SI lesion in the splenium (white arrow) and other multifocal nodular high SI lesions in both thalami, right caudate nucleus, and periventricular white matter of the left parietal lobe (black arrows), suggesting multiple sclerosis. Follow-up MRI (**D–F**), after 17 months, shows resolution of signal abnormalities in the splenium on all sequences.

Note.—ADC = apparent diffusion coefficient, DWI = diffusion-weighted imaging, SI = signal intensity, T2-WI = T2-weighted image

totoxic lesions in the brain and frequently affect the median aspect of the splenium of the CC (10). Tada et al. (11) stated that transient restricted diffusion of the splenium might be related to an influx of inflammatory cells and macromolecules combined with related cytotoxic edema. The vulnerability of the splenium of the CC can be explained by viral antigens having specific affinities for receptors on splenial axons or the myelin sheaths surrounding them, but this theory (11) lacks pathologic correlation.

Mild cytotoxic edema can show normal ADC due to its small size or combination with vasogenic edema (12). Our patient (case 5) showed iso-SI on an ADC map (Fig. 4B). As the ADC

signal subsequently changes from dark to bright, 7-10 days after clinical onset, we believed the brain MRI of our patient might have been performed at an increasing phase of ADC value.

MS is the most common demyelinating disease of unknown cause that characteristically involves the periventricular white matter, internal capsule, CC, and pons (9, 12). Because the CC is the most heavily myelinated bundle within the brain, it is a preferred target of the demyelinating processes (9, 16, 17). On DWI, the acute phase of MS may show increased ADC, due to vasogenic edema and myelin destruction with axonal preservation, or decreased ADC due to intramyelinic edema (12). Otherwise, chronic MS plaques do not show restricted diffusion (12). In-

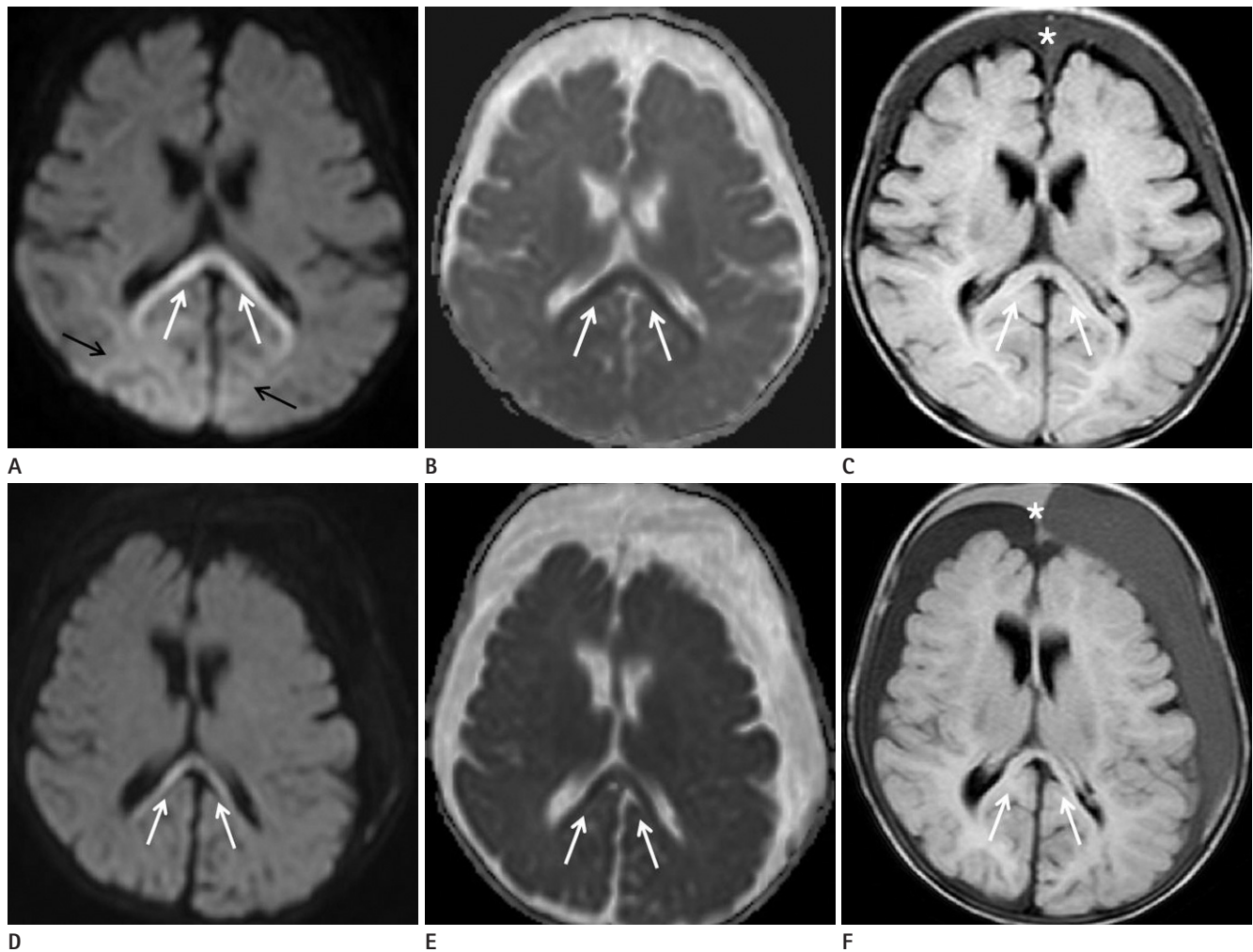


**Fig. 6.** A 3-month-old girl with episodes of seizures (case 7). Initial MRI (**A-C**) shows bilateral linear bright SI lesions (arrows) on DWI (**A**) and low SI (arrows) on an ADC map (**B**) in the splenium of the corpus callosum, crossing the midline. Ill-defined high SI lesions on DWI, with subtle cortical sulcal effacement, are seen in both occipital lobes (black arrows) without low SI on ADC map, suggesting vasogenic edema. FLAIR imaging (**C**) shows high SI in the splenium (arrows) and crescentic subdural hygroma in both frontotemporoparietal regions (asterisk). Subdural hygroma on conventional T1-WI and T2-WI (not shown) was well-depicted, showing iso-SI to the cerebrospinal fluid. After 1 month, the girl revisited our hospital for general weakness. Follow-up MRI (**D-F**) shows that the bilateral linear lesions in the splenium are persistent (arrows) on DWI (**D**) and an ADC map (**E**). FLAIR imaging (**F**) shows the amount of subdural hygroma in both frontotemporoparietal regions has increased, with complicated hemorrhage (asterisk). A burr-hole craniotomy was performed for drainage of the subdural hygroma.  
 Note.—ADC = apparent diffusion coefficient, DWI = diffusion-weighted imaging, FLAIR = fluid-attenuated inversion-recovery, SI = signal intensity, T1-WI = T1-weighted image, T2-WI = T2-weighted image

tramyelinic edema occurs in the myelin sheath itself and/or in the intramyelinic cleft. Some of the intramyelinic edema is reversible, probably because it is located primarily in the intramyelinic cleft. Another possible explanation is inflammatory infiltration. A DWI study of MS revealed decreased ADC values, in some lesions, from MS, and the influx of inflammatory cells and macromolecules was postulated to have caused the decreased ADC values. A decreased ADC value in the splenium of the CC may be a result of inflammation, and the ADC may return to normal if the cause resolves quickly (13).

Several limitations of this study should be noted. First, it was a retrospective study including a small number of cases. Second, although the clinical significance of these signal changes in the CC should be determined in follow-up studies, follow-up MRI scans were performed only in a few pediatric patients, which might have an influence on the reliability of the results. Third, because this was a retrospective study, the timing of the initial imaging scans varied depending on the child's status. To advance efforts toward improving the outcome of patients with lesions of the CC, a larger prospective study or case-control study

is needed for exclusion of the aforementioned biases. Fourth, the ADC values were not measured. Finally, a lack of histopathologic correlation does not allow us to confirm our findings. Most of the pathogenesis, and the nature of restricted diffusion, are theoretical, and because the clinical and radiologic findings were rapidly resolved in most of the patients, they did not require an invasive diagnostic examination.

Rapid resolution of clinical and radiologic findings suggests a good prognosis. Clinical courses and outcomes were good in five of the seven cases reported here (cases 1-5). These patients showed complete resolution of restricted diffusion in the CC, on follow-up MR examinations (17 days, 1 month, 2 months, 6 months, and 17 months after the initial examination, respectively). Although the restricted diffusion was reversible in our patient with MS (case 6) (Fig. 5), rehabilitation was necessary because of his motor weakness. This can be explained by a relapsing and remitting course of the multiple sclerosis, and severe neurologic sequelae were not observed. Thus, reversible restricted diffusion is suggested to imply a less severe course and a good outcome. Conversely, in the last case (case 7) (Fig. 6), restricted diffusion in the CC was persistent, on follow-up MRI, after 1 month; the patient's outcome was poor. After her seizure was controlled following administration of phenobarbital and phenytoin, and she recovered clinically, she revisited our hospital for general weakness. The subdural hygroma in both frontotemporoparietal regions had increased with complicated hemorrhage. A burr-hole craniotomy was performed for drainage of subdural hygroma. Such a severe clinical outcome was also previously reported in a patient with osmotic myelinolysis; this particular patient did not show reversible lesions (18). Thus, the follow-up MRI can confirm the irreversibility of callosal lesions and may be helpful in predicting patients' clinical outcomes and prognoses. Additional parenchymal lesions with restricted diffusion, however, do not necessarily suggest a severe outcome or predict irreversible MRI findings. Further investigations are required in order to assess the association between additional parenchymal lesions and clinical outcomes.

In conclusion, reversible restricted diffusion in the CC can develop in various diseases, with various pathogeneses. Rapid resolution of the clinical and radiologic findings suggests a good prognosis, and follow-up MRI could confirm the reversibility or irreversibility of callosal lesions. Knowledge of the MRI findings

and associated conditions might be helpful in predicting patients' conditions and clinical outcomes.

## REFERENCES

1. Matsukawa H, Shinoda M, Fujii M, Takahashi O, Yamamoto D, Murakata A, et al. Genu of corpus callosum in diffuse axonal injury induces a worse 1-year outcome in patients with traumatic brain injury. *Acta Neurochir (Wien)* 2011; 153:1687-1693; discussion 1693-1694
2. Kim SS, Chang KH, Kim ST, Suh DC, Cheon JE, Jeong SW, et al. Focal lesion in the splenium of the corpus callosum in epileptic patients: antiepileptic drug toxicity? *AJNR Am J Neuroradiol* 1999;20:125-129
3. Prilipko O, Delavelle J, Lazeyras F, Seeck M. Reversible cytotoxic edema in the splenium of the corpus callosum related to antiepileptic treatment: report of two cases and literature review. *Epilepsia* 2005;46:1633-1636
4. Mirsattari SM, Lee DH, Jones MW, Blume WT. Transient lesion in the splenium of the corpus callosum in an epileptic patient. *Neurology* 2003;60:1838-1841
5. Matsubara K, Kodera M, Nigami H, Yura K, Fukaya T. Reversible splenial lesion in influenza virus encephalopathy. *Pediatr Neurol* 2007;37:431-434
6. Fukuda S, Kishi K, Yasuda K, Sejima H, Yamaguchi S. Rotavirus-associated encephalopathy with a reversible splenial lesion. *Pediatr Neurol* 2009;40:131-133
7. Ogura H, Takaoka M, Kishi M, Kimoto M, Shimazu T, Yoshioka T, et al. Reversible MR findings of hemolytic uremic syndrome with mild encephalopathy. *AJNR Am J Neuroradiol* 1998;19:1144-1145
8. Kim JH, Choi JY, Koh SB, Lee Y. Reversible splenial abnormality in hypoglycemic encephalopathy. *Neuroradiology* 2007;49:217-222
9. Bourekas EC, Varakis K, Bruns D, Christoforidis GA, Baujan M, Slone HW, et al. Lesions of the corpus callosum: MR imaging and differential considerations in adults and children. *AJR Am J Roentgenol* 2002;179:251-257
10. Grünbaum B, Salzer H, Nasel C, Lernbass I. Reversible cytotoxic oedema in the splenium of the corpus callosum related to tetracycline therapy. *Pediatr Radiol* 2010;40: 1693-1695

11. Tada H, Takanashi J, Barkovich AJ, Oba H, Maeda M, Tsukahara H, et al. Clinically mild encephalitis/encephalopathy with a reversible splenial lesion. *Neurology* 2004;63:1854-1858
12. Karaarslan E, Arslan A. Diffusion weighted MR imaging in non-infarct lesions of the brain. *Eur J Radiol* 2008;65:402-416
13. Takanashi J, Maeda M, Hayashi M. Neonate showing reversible splenial lesion. *Arch Neurol* 2005;62:1481-1482; author reply 1482
14. Kubota T, Kidokoro H, Ito M, Oe H, Hattori T, Kato Y, et al. Diffusion-weighted imaging abnormalities in the corpus callosum after neonatal seizure: a case report. *Brain Dev* 2008;30:215-217
15. Takanashi J, Hirasawa K, Tada H. Reversible restricted diffusion of entire corpus callosum. *J Neurol Sci* 2006;247:101-104
16. Sigal T, Shmuel M, Mark D, Gil H, Anat A. Diffusion tensor imaging of corpus callosum integrity in multiple sclerosis: correlation with disease variables. *J Neuroimaging* 2012;22:33-37
17. Simon JH, Holtås SL, Schiffer RB, Rudick RA, Herndon RM, Kido DK, et al. Corpus callosum and subcallosal-periventricular lesions in multiple sclerosis: detection with MR. *Radiology* 1986;160:363-367
18. Maeda M, Tsukahara H, Terada H, Nakaji S, Nakamura H, Oba H, et al. Reversible splenial lesion with restricted diffusion in a wide spectrum of diseases and conditions. *J Neuroradiol* 2006;33:229-236

## 소아 질환에서 나타나는 뇌량의 가역적 확산강조영상 소견<sup>1</sup>

김원경<sup>1</sup> · 홍현숙<sup>1</sup> · 이아름<sup>1</sup> · 차장규<sup>1</sup> · 이해경<sup>1</sup> · 배원경<sup>2</sup>

**목적:** 소아 환자에서 뇌량에 나타나는 가역적 확산강조영상 소견과 임상 양상을 평가하고 가능한 발병 기전을 알아보고자 하였다.

**대상과 방법:** 2007년부터 2011년까지 뇌량의 가역적 신호강도 변화를 보인 총 7명의 소아 환자들(남아 5명, 여아 2명; 연령 범위 0~19세; 평균 연령 8.6세)을 대상으로 하였고, MRI 소견, 임상 양상, 예후를 후향적으로 평가하였다.

**결과:** 뇌량의 신호강도 변화와 관련된 질병이나 상태는 외상( $n = 3$ ), 신생아 경련( $n = 1$ ), 임상적으로 의심되는 뇌병증( $n = 1$ ), 다발성경화증( $n = 1$ ), 그리고 경련과 동반된 뇌경막하수종( $n = 1$ )이었다. 뇌량의 신호강도 변화 위치는 splenium과 genu ( $n = 2$ ), splenium과 body ( $n = 1$ ), 그리고 splenium 단독( $n = 4$ )이었으며 모양은 4명의 환자에서 원형 혹은 타원형으로, 나머지 3명의 환자에서 선형으로 보였다. 추적 MRI에서 6명은 뇌량의 확산강조영상과 확산계수지도에서의 신호강도 변화가 소실되었으나 1명은 지속적으로 관찰되었다. 가역적 신호강도 변화를 보인 6명에서는 좋은 예후를 보였으나 지속적으로 신호강도 변화가 관찰된 1명은 나쁜 예후를 보였다.

**결론:** 뇌량의 가역적 확산강조영상 소견은 여러 질병에서 보일 수 있으며 MRI 소견과 이에 연관된 질병들을 아는 것이 환자의 상태와 예후를 예측하는 데 도움을 줄 수 있다.

<sup>1</sup>순천향대학교 의과대학 부천병원 영상의학과학교실, <sup>2</sup>순천향대학교 의과대학 천안병원 영상의학과학교실